The forward glory effect in the differential cross sections measured below E_{lab} = 50 eV for the one-electron capture process in N^{5+} - He collisions

Yoh Itoh

Physics laboratory, Faculty of science, Josai University, Saitama 350-0295, Japan

E-mail: yitoh@josai.ac.jp

Abstract

A crossed-beam apparatus was used to measure the relative state-selective differential cross sections for the one-electron capture process in the N^{5+} - He system from θ_{lab}= –3° to 21° at E_{lab} = 27.5 and 47.5 eV. The main reaction channel was found to be N^{5+} ($1s^2$ ^{1}S) + He → N^{4+} ($1s^2$ 3s ^{2}S) + He^+ + 16.8 eV. The differential cross section for this channel is pronounced at θ_{cm} = 0, and it shows another peak at a certain angle that depends on the collision energy. The O^{5+} - He system at E_{lab} = 47.5 eV was measured for comparison. The differential cross section for the main reaction channel: O^{5+} ($1s^2$ 2s ^{2}S) + He → O^{4+} ($1s^2$ 2s3p ^{1,3}P) + He^+ + 17 eV, is zero at θ_{cm} = 0, and it shows only a single peak at θ_{cm} = 0.314 rad. The structures observed in the N^{5+} - He system were analyzed using the classical deflection function based on *ab initio* potentials. The peak observed at θ_{cm} = 0 is assigned to the forward glory effect and the second peak to the inelastic rainbow effect.

Keywords: one-electron capture, multiply charged ion, differential cross section, interaction potential, glory effect, rainbow effect

PACS: 34.70.+e

1. Introduction

Within a classical or a semi-classical picture for low energy collisions, the one-electron capture reaction including multiply-charged ions of the type:

$$A^{n+} + B \rightarrow A^{(n-1)+} + B^{+} + \Delta E, \qquad (1)$$

where ΔE stands for the exothermicity, is well understood to occur around the crossing point of the interaction potentials relevant to the reaction. Two pathways are considered for the reaction: One reaction occurs at the first crossing, while the other occurs at the second crossing. A study of this process thus provides us a good chance to gain information on the transition probabilities at the crossing points and the interaction potentials. Measurements of state-selective differential cross sections are a powerful means for this purpose, but there exist fewer reports than those on the absolute cross sections. A two-state model is often applied to the analysis of the differential cross sections, and the observed structures were interpreted using the ideas obtained from the analysis of elastic scattering such as the rainbow and glory effects, and the Stückelberg oscillations (see, e.g. [1 - 6]).

One of the simplest collision systems including multiply-charged ions is the N^{5+} ion on the He target; the electronic configuration of the projectile in the ground state and that of the target are both $1s^2$ ($^1S_0$), and the symmetry of the molecular state concerned with the collision is only $^1\Sigma^+$ at low energies. State-selective total cross sections for the one-electron capture process determined by the use of vacuum ultraviolet (VUV) spectroscopy were reported by Cotte *et al* [7] and Dijkkampt *et al* [8] above E_{lab} = 15 keV. Their measurements report that the main reaction channel is N^{5+} ($1s^2$ ^1S) + He $\rightarrow$ N^{4+} ($1s^2$ $3l$) + He^+ and that the reaction to the N^{4+} ($1s^2 3s$ ^2S) is the dominant channel among the possible reaction channels at the lowest collision energy. A theoretical study by Bacchus-Montabonel [9] based on the potentials obtained by *ab initio* calculation [10] reproduced the experimental findings very well. Nearly identical results were recently reported by Liu *et al* [11] .

When the differential cross sections are studied in isoionic systems, one can observe a systematic change in the cross sections due to the difference in their interaction potentials. When a one-electron capture reaction occurs in the incoming channel of the trajectory, the ion trajectory is mainly determined by the Coulomb repulsive force between the projectile ion that captures an electron and the product ion. The trajectory in this case may be nearly identical to an isoionic system, so that the contribution to the cross section is also similar. While the reaction happens in the outgoing channel of the trajectory, the deflection angle is expected to be

different due to the difference in the potentials inside the crossing point. Therefore, this contribution should clearly influence the differential cross sections.

Shimakura *et al* [12] reported a theoretical study of the one-electron capture process in O^{5+} - He collisions, which is an isoionic system of the N^{5+} - He, based on *ab initio* potentials. They showed that the dominant reaction channel is $O^{5+}(1s^2 2s) + He \rightarrow O^{4+}(1s^2 2s3l) + He^+$ and that their result agrees well with the experimental findings of Kimura *et al* [13] obtained at E_{lab}= 5.2 keV. It should be noted that the interaction potentials relevant to the reactions are all repulsive, while a shallow well exists in the theoretical potential that describes the initial channel in N^{5+} ($1s^2\ ^1S$) + He [10].

The importance of the measurements of differential cross sections for an electron capture process at low energies is, as clearly stated in [2 - 4], that the angular distribution of the scattered ions depends strongly on the nature of the interaction potentials and that it becomes more prominent as the collision energy is lowered. The purpose of the present paper is to show the difference observed in the state-selective differential cross sections in the N^{5+} - He and O^{5+} - He systems measured below E_{lab} = 50 eV.

2. Experimental

We combined the technique of translational energy spectroscopy with the crossed-beam method for the measurements of relative differential cross sections. The apparatus and the experimental procedures were reported in detail [14, 15]. Briefly, multiply charged ions created by a small electron-beam ion-source (EBIS) were extracted and mass-selected by a Wien-filter. Mass-selected ions were energy-selected by a double hemispherical energy selector. The transmission energy of the selector was 48*q* eV, and the energy spread of the ion beam was estimated to be 0.3*q* eV at the full width at half maximum (FWHM), where *q* indicates the charge number of the ions. The mass- and energy-selected ions were decelerated to the collision energy and crossed with a supersonic nozzle beam at the right angle. The beam intensity at the collision centre was less than 0.1 pA. State-selective differential cross sections were determined by measuring the kinetic energy of the scattered ions using a one-dimensional position-sensitive energy analyser, and the angular dependence of the scattered ions were determined from the ion intensity recorded on the energy spectra obtained by rotating the analyser around the collision centre. The in-plane configuration, where the ion detector was rotated in the plane of the beams, was applied to precisely determine the collision kinematics. The overall energy resolution of the

present measurements was about 1.0q eV, and the angular resolution was about ± 0.8°. It took about 1.5 to 2 h to obtain an energy spectrum at each angle setting.

Accurate determination of the collision energy is crucially important for the assignment of the reaction channels from the energy measurements of the product ions. For this purpose, we measured the elastically scattered ions simultaneously, because the energy- and angular-dependences of elastic scattering are uniquely determined by the scattering geometry. We assumed the (5/2) kT limit [16], where the nozzle temperature T was 300 K, to estimate the velocity of the target beam for use in the calculation of the kinematics. The measured energy and angular dependences of the elastically scattered ions were compared with the calculated ones obtained by changing the impact energy so as to reproduce the results. The accuracy of the collision energy determined in this way was cross-checked by using the ions with different charge states retaining the ion-source parameter constant. The error in the collision energy determination was estimated to be less than ± 0.3q eV.

We observed strong background ions at the energy positions where the signals due to the one-electron capture reaction were expected to appear in the forward direction. These ions were ascribed to those produced by collisions with the background gas, the remaining target gas, and the edge scattering. Therefore, special care was taken to distinguish the signal from the background noise, which was subtracted by the following procedures: (1) A series of spectra using the supersonic target beam was recorded. (2) The target beam was stopped, and the helium gas was put into the scattering chamber directly from a separate gas-inlet system up to the same pressure when the target beam was running. (3) The counts of the noise component measured under these conditions were subtracted from those of the signal component. The example of the spectra obtained in this procedure is shown in figures 3(*a*) and (*b*).

3. Results and discussion

3.1. Final-state analysis for the one-electron capture reaction in N^{5+} - He

In figure 1(*a*), the ion energy spectra measured from θ_{lab} = 3.0° to 21° at intervals of 0.3° are shown in a two-dimensional diagram. The contour interval is about 7% of the maximum ion counts. In the individual energy spectra obtained at θ_{lab} = 3.9° and 12.0° shown in figures 1(*b*) and (*c*), respectively, noise counts were subtracted from the measured spectra, but no further data treatment was made. The curve labeled E in figure 1(*a*) shows the calculated positions for the elastically scattered N^{5+} ions on the He target at the collision energy of E_{lab} = 47.5 eV. This curve was calculated so as to reproduce the measured angular dependence of the elastically scattered ions by changing the collision energy as a parameter.

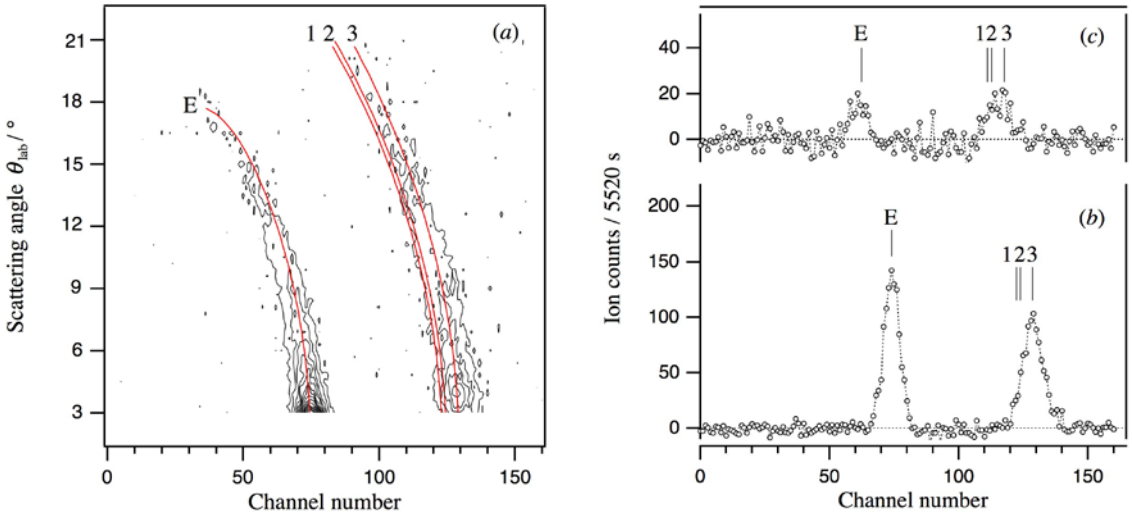

Figure 1. (*a*) Energy spectra of the scattered ions in N^{5+} - He system at E_{lab} = 47.5 eV. Measured spectra at different angles are shown in a two-dimensional plot as a function of the scattering angle. The channel number corresponds to the kinetic energy of the ions; the increment of energy is about 0.103*q* eV. curve E: calculated position for the elastically scattered ions. curve 1, 2, 3 : calculated positions for the one-electron captured signals to the final states, N^{4+} ($1s^2$ 3d ^{2}D), N^{4+} ($1s^2$ 3p ^{2}P) and N^{4+} ($1s^2$ 3s ^{2}S), respectively. (*b*) Individual energy spectra obtained at θ_{lab} = 3.9° and (*c*) at θ_{lab} = 12.0°.

The curves labeled 1 to 3 correspond to the reaction channels (2) to (4), respectively:

$$N^{5+}(1s^2\ {}^1S) + He(1s^2\ {}^1S)$$

$$\rightarrow N^{4+}(1s^2 3d\ {}^2D) + He^{+}(1s\ {}^2S) + 13.2\ eV\ , \qquad (2)$$

$$\rightarrow N^{4+}(1s^2 3p\ {}^2P) + He^{+}(1s\ {}^2S) + 14.1\ eV, \qquad (3)$$

$$\rightarrow N^{4+}(1s^2 3s\ {}^2S) + He^{+}(1s\ {}^2S) + 16.8\ eV. \qquad (4)$$

The observed peak position coincides with the reaction channel (4). Though the energy resolution of the present measurement was not sufficient to clearly separate the reaction channels (2) to (4), the apparent energy width of the peak for the elastic scattering is slightly narrower than that of the one-electron capture peak. This is mainly due to the experimental settings, i. e., the kinetic energies of the ions with different charge states were measured by an electrostatic energy-analyser. In figure 1(*b*), for example, the FWHM of the elastic peak was 7.08 ± 0.17 channel; this corresponds to 3.63 ± 0.09 eV, while that for the reaction channel was 8.81 ± 0.26 channel, 3.61 ± 0.11 eV. As they were found to be nearly equal, we attempted to deconvolute the intensities for these channels, but no trustable results were obtained. The sum of the cross sections for channels (2) and (3) was estimated to be less than 5 % of channel (4). Hence, only channel (4) was taken into account in the following analysis.

To the best of our knowledge, no state-selective measurements comparable with the present results are available; the present results generally agree with those obtained at higher energy regions. For example, Okuno *et al* [17] reported the energy gain spectrum measured by translational spectroscopy at E_{lab} = 10 keV and $\theta_{lab} = 0^{o}$. The main reaction channel was found to be the $N^{4+}(1s^2\ 3l)$ states, the peak position being located close to the level that was ascribed to channel (4). The absolute state-selective cross sections were measured by Beijers *et al* [18] in the range of E_{lab} = 686 eV to 20 keV, where VUV photon emission spectroscopy was employed. At the lowest collision energy of their measurements, the cross section for channel (4) was reported to be 10.8×10^{-16} cm^2, while that for channel (3) was 4.29×10^{-16} cm^2. Both cross sections were shown to increase with the increase in the collision energy. Since the energy dependence of the cross section for channel (3) was stronger than that for channel (4), the relative importance of channel (4) is expected to be enhanced at lower collision energies. This trend supports our assignment discussed above.

3.2. Final-state analysis for the one-electron capture reaction in O^{5+} - He

The ion energy spectra measured from θ_{lab} = 3.0° to 21° at intervals of 0.3° are shown in figure 2(*a*) in a two-dimensional diagram. The contour interval is about 7% of the maximum ion counts. The individual energy spectra obtained at θ_{lab} = 4.8° and 12.0° are shown in figures 2(*b*) and (*c*), respectively. The curve labeled E shows the calculated positions for the elastically scattered O^{5+} ions on the He target at E_{lab} = 47.5 eV. We performed the measurements with the same condition applied for those in the N^{5+} - He collisions. Therefore, we simply calculated the curve E applying the same collision energy and found that the curve reproduced the experimental results well.

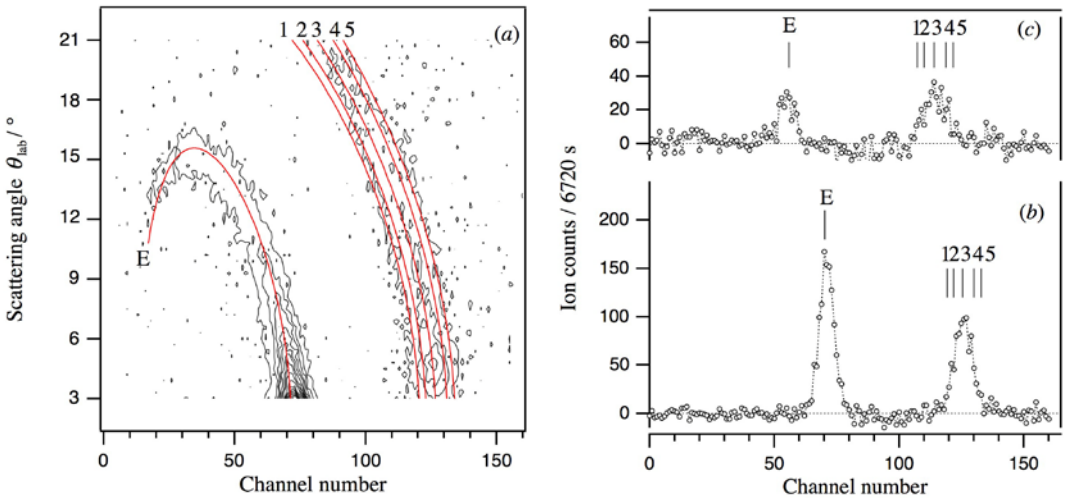

Figure 2. (*a*) Energy spectra of the scattered ions in the O^{5+} - He system at E_{lab} = 47.5 eV. Measured spectra at different angles are shown in a two-dimensional plot as a function of the scattering angle. Curve E: calculated position for the elastically scattered ions. Curves 1, 2, 3, 4, 5: calculated positions for the one-electron captured signals to the final states, $O^{4+}(1s^2 2s3d\ ^1D)$, $O^{4+}(1s^2 2s3d\ ^3D)$, $O^{4+}(1s^2 2s3p\ ^{1,3}P)$, $O^{4+}(1s^2 2s3s\ ^1S)$ and $O^{4+}(1s^2 2s3s\ ^3S)$, respectively. (*b*) Individual energy spectra obtained at θ_{lab} = 4.8° and (*c*) at θ_{lab} = 12.0°.

The curves labeled 1 to 5 correspond to the following reaction channels, respectively:

$$O^{5+}(1s^2 2s\ ^2S) + He(1s^2\ ^1S)$$

$$\rightarrow O^{4+}(1s^2 2s3d\ ^1D) + He^+(1s\ ^2S) + 13.4\ eV\ , \quad (5)$$

$$\rightarrow O^{4+}(1s^2 2s3d\ ^3D) + He^+(1s\ ^2S) + 14.8\ eV, \quad (6)$$

$$\rightarrow O^{4+}(1s^2 2s3p\ ^{1,3}P) + He^+(1s\ ^2S) + 17\ eV, \quad (7)$$

$$\rightarrow O^{4+}(1s^2 2s3s\ ^1S) + He^+ (1s\ ^2S) + 19.7\ \text{eV}, \quad (8)$$

$$\rightarrow O^{4+}(1s^2 2s3s\ ^3S) + He^+ (1s\ ^2S) + 21.5\ \text{eV}. \quad (9)$$

The peak position for the one-electron captured signal coincides with the energy position for the reaction channel (7) for all the angular range measured. The FWHM of the elastic peak was 3.54 ± 0.08 eV and that for the reaction channel was 3.60 ± 0.12 eV in figure 2(*b*). The peak widths for both signals are again nearly equal; therefore, the reaction channel (7) is concluded to be the dominant process at this collision energy.

Kimura *et al* [13] measured an energy gain spectrum at E_{lab} = 5.2 keV and θ_{lab} = 0º and suggested that the final states are channel (7) or (8) and the cross section for channel (6) is very small. Their results were found to be consistent with the theoretical work of Shimakura *et al* [12], but somewhat different results were reported by Bangsgaard *et al* [19] from the energy gain spectrum measured at E_{lab} = 500 eV and θ_{lab} = 0º. According to their analysis, the cross section for channel (6) was nearly equal to that for channel (7), and those for channels (8) and (9) were much smaller. The reason for this discrepancy is not clear at present.

3.3. Ion spectra observed around θ_{lab} = 0°

The ion spectra due to the one-electron capture process obtained in the forward direction, shown in figures 3(*a*) and (*b*), were measured in the N^{5+} - He collisions at E_{lab} = 47.5 eV and θ_{lab} = – 0.3°. From figure 3(*b*), obtained after the noise subtraction reported in section 2, we have confirmed that the N^{4+} ion signal observed in the forward direction is a true signal created by the one-electron capture process in the N^{5+} - He collision.

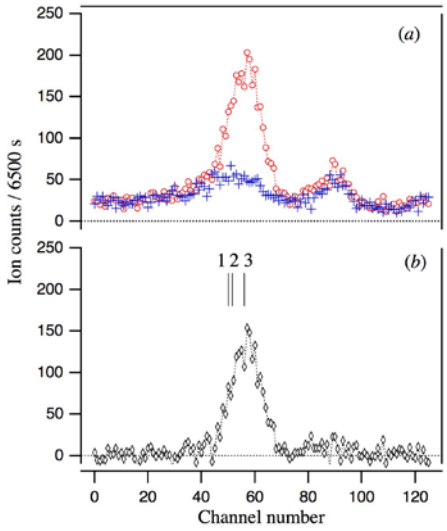

Figure 3. (*a*) Energy spectra of the scattered ions in the N^{5+} - He collisions at E_{lab} = 47.5 eV measured at θ_{lab} = – 0.3°. Ion signals (○) with target beam, and (+) when the target beam was stopped and the background gas was introduced. (*b*) a background-subtracted spectrum. See figure 1 for the meaning of the labeled bars.

The same procedure was applied for the forward scattering in the O^{5+} - He collisions. Two spectra with the target beam and with the background gas were found to be totally identical. Therefore, we emphasize that there exists no signal for the one-electron capture reaction around 0° in the O^{5+} - He collisions.

3.4. Angular distributions of the scattered ions and differential cross sections

The angular distribution of the scattered ions for the one-electron capture process in the N^{5+} - He collisions at E_{lab} = 47.5 eV is shown in figure 4. The scattered ion counts were determined with the aid of a curve-fitting program used to integrate the ion counts under the peak in the spectra obtained at different scattering angles. The error bar shows the sum of the statistical error and the inaccuracy of this curve-fitting procedure.

Two peaks are observed in the angular distribution. The first one is located around θ_{lab} = 0°; the peak position is slightly shifted to the negative side. This is the typical kinetic effect for the exothermic reactions, where the scattering angle in the centre-of-mass system is zero, and this small shift is made detectable by the use of a supersonic nozzle beam for the target preparation. The second peak is located around θ_{lab} = 3.9°. The measured angular profile of the primary beam, also shown in figure 4, is equivalent to the overall angular resolution of the present

measurements, ± 0.8°. The angular widths of the two peaks are found to be slightly broader than that of the primary beam; therefore, the actual width of the peaks is likely to be much narrower than that measured.

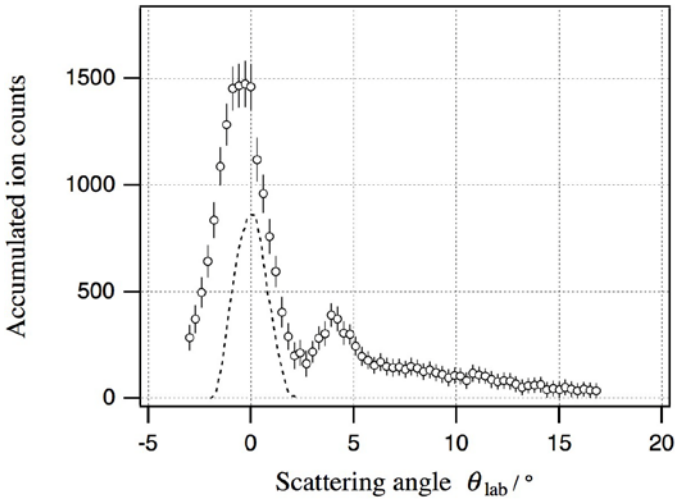

Figure 4. ○: Angular distribution of the scattered ions corresponding to the one-electron capture reaction in the N^{5+} - He system at E_{lab} = 47.5 eV. The dashed curve shows the angular profile of the primary beam.

By application of equations (8) and (13) in [20], the angular distribution of the ions shown in figure 4 is converted to the relative differential cross section in the centre-of-mass system. In figure 5(*a*), the differential cross for the reaction channel (4) at E_{lab} = 47.5 eV (E_{cm} = 10.6 eV), is shown. As we measured only relative cross sections, the maximum intensity is normalized to unity. Note that the definition of the differential cross section in this figure is $d\sigma / d\Omega$, instead of $d\sigma / d\theta = 2 \pi \sin \theta \; d\sigma / d\Omega$. The relative differential cross section determined at E_{lab} = 27.5 eV (E_{cm} = 6.11 eV) is also shown in figure 5(*b*). Two prominent structures are seen in these differential cross sections. One is the large cross section at θ_{cm} = 0 rad, and the other is the second maximum observed at θ_{cm} = 0.242 rad, E_{cm} = 10.6 eV and θ_{cm} = 0.338 rad, E_{cm} = 6.11 eV.

The relative differential cross section in the O^{5+} - He collisions at E_{lab} = 47.5 eV (E_{cm} = 9.50 eV) is shown in figure 6. Only a single maximum is observed at θ_{cm} = 0.314 rad, and the cross section decreases with the increase in the scattering angle with little structure.

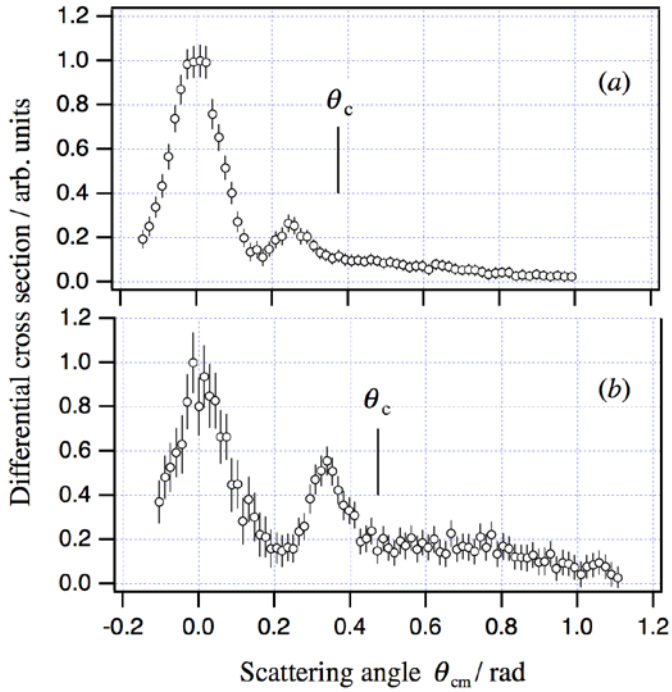

Figure 5. (*a*) Relative differential cross section in the centre-of-mass system for the one-electron capture reaction: $N^{5+}(1s^2\ ^1S) + He \rightarrow N^{4+}(1s^2\,3s\ ^2S) + He^+ + 16.8$ eV, at $E_{cm} = 10.6$ eV, and (*b*) at $E_{cm} = 6.11$ eV. The critical angle θ_c is indicated; see text.

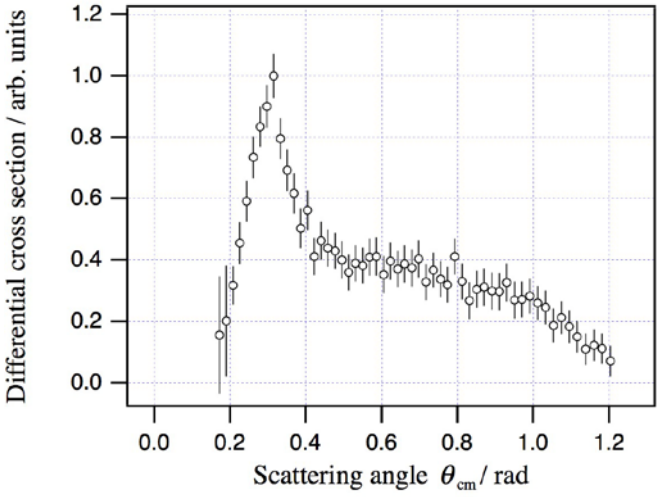

Figure 6. Relative differential cross section in the centre-of-mass system for the reaction $O^{5+}(1s^2 2s\ ^2S) + He \rightarrow O^{4+}(1s^2 2s3p\ ^{1,3}P) + 17$ eV, at $E_{cm} = 9.50$ eV.

3.5. Comparison of the angular distributions with those reported at higher energy regions

The angular scatterings for the one- and two-electron capture reactions in O^{5+} - He were studied by Sobocinski *et al* [21] in the energy range from E_{lab} = 100 to 2500 eV to extract the information on the transition probabilities for the processes. They measured the angular distribution of the recoil product-ions, He^{+} and He^{2+}, and reported the total differential cross section, i.e., the sum of the one- and two-electron capture reactions, at E_{lab} = 100 eV as a function of the detection angle measured from the projectile beam direction. The differential cross section showed very little angular dependence and had a large value at 90º that corresponded to the forward scattering of the O^{4+} or O^{3+} ions. This tendency does not agree with the present results. Though the reason for this disagreement is uncertain at present, it is probably due to the experimental settings that they employed, especially an effusive source was used for the target beam. Since the angular divergence of an effusive beam is larger than that produced by a supersonic expansion, the angular resolution in the centre-of-mass system could be degraded. The disagreement might also be due to the angular step of the measurements. The cross sections were measured at intervals of θ_{lab} = 10° to 20°; this might be too coarse to detect the fine angular dependence.

Total differential cross sections, $d\sigma / d\theta$, including one- and two-electron capture processes without a final-state analysis were also reported by Waggoner *et al* [2] both for the N^{5+} and O^{5+} on He systems at E_{lab} ~ 7.5 keV. They observed strong forward peaking in the differential cross sections for both systems. The peaks were located in the angles smaller than the so-called critical angle θ_c [22, 23]; then they assigned this forward peak to the scattering that corresponds to the one-electron capture process that happened in the outgoing part of the trajectory. They observed a single peak in the differential cross section in the N^{5+} - He collisions, while two peaks were observed in the O^{5+} - He case, both in angles smaller than the critical angle. They temporally assigned the peak observed at a smaller angle in the O^{5+} - He collision was due to the glory effect (see, e. g. [24]). This point will be further discussed in the next subsection.

3.6. Origin of the maxima in the observed cross section

To understand the origin of the maxima observed in the differential cross sections semi-quantitatively, we applied the classical trajectory analysis using model potentials based on a theoretical calculation.

In the N^{5+} - He collisions, only the reaction channel (3) can be regarded as the dominant

process, as discussed in subsection 3.1; hence we applied the following two-state approximation. Atomic units are used hereafter unless indicated otherwise. We set up a Morse-type potential for the initial channel by fitting the potential energies obtained in the *ab initio* calculations reported by Bacchus-Montabonel [10]:

$$V_{\text{ini}}(r) = 0.071[1 - \exp\{-0.731(r - 4.0)\}]^2 - 0.071. \quad (10)$$

We considered only the Coulomb repulsive potential and the exothermicity for the one-electron capture channel:

$$V_{\text{final}}(r) = \frac{4}{r} - 0.6156. \quad (11)$$

The model potentials used are shown in figure 7, and the deflection function calculated using these potentials for the collision at E_{lab} = 27.5 eV (E_{cm} = 6.11 eV) is shown in figure 8. The upper half of the curve shown in figure 8 corresponds to the deflection function when the one-electron capture process happens in the incoming part of the trajectory. In this case, the ion trajectory is governed by the Coulomb repulsion force; thus the deflection angle is always positive. The lower half of the curve represents the reaction that occurs in the outgoing part of the trajectory. In this situation, the ion trajectory is determined by the attractive force until the second crossing, after passing through the crossing point; it is controlled by the Coulomb force. Therefore, the deflection angles become zero or negative at certain impact parameters due to the competition of the attractive and repulsive forces. In figure 8, we find that the cancellation of the attractive and repulsive forces occurs at impact parameters b = 4.3 and b = 6.0, which result in $\theta_{\text{cm}} = 0$.

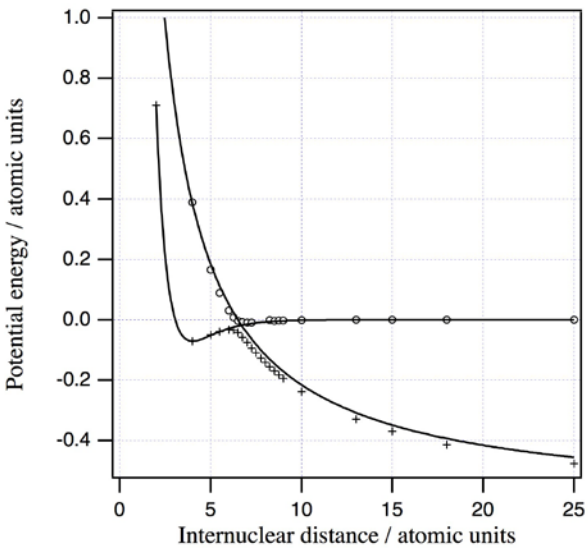

Figure 7. Curves: model potentials used to calculate the deflection function in the N^{5+} - He system. ○, + : the potential energies reported by Bacchus-Montabonel [10].

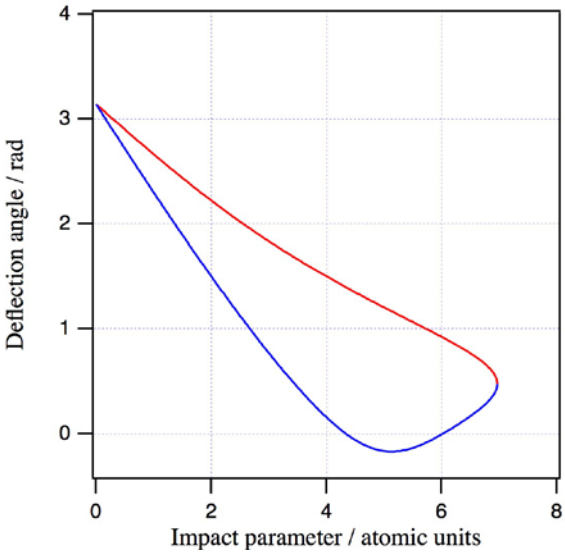

Figure 8. Deflection function for the one-electron capture reaction in the N^{5+} - He system at E_{lab} =27.5 eV (E_{cm} = 6.11 eV).

The upper and lower curves meet at b = 7.0, where the deflection angle in this condition is 0.473 rad. The scattering angle determined by this condition is called the critical angle θ_c [22, 23]. The structures in the differential cross sections observed below θ_c are ascribed to the reactions that happen in the outgoing part of the trajectory, while those observed beyond θ_c are mainly ascribed to those in the incoming part. When the collision energy is E_{lab} = 47.5 eV (E_{cm} = 10.6 eV), the critical angle is calculated to be 0.374 rad at b = 6.85. These critical angles are indicated in figures 5(*a*) and (*b*), where the observed peaks are located inside the critical angles.

The classical differential cross section for the elastic collision can be evaluated by [24]

$$\frac{\mathrm{d}\sigma}{\mathrm{d}\Omega} = \sum_j \frac{b_j}{\sin\theta}\left|\frac{\mathrm{d}\theta}{\mathrm{d}b_j}\right|^{-1}, \qquad (12)$$

where b_j is the possible impact parameter to result in the same deflection angle θ in the centre-of-mass system. For the electron capture process, differential cross sections are often evaluated by the product of the elastic cross section and the transition probability for the

reaction [3]. The transition probability, often evaluated by the Landau-Zener formula, scarcely depends on the impact parameter unless the impact parameters are very close to the crossing radius [25]. Therefore, the overall angular dependence of the differential cross section for the reaction can be determined by the elastic differential cross sections to the limit of adequacy of this classical treatment.

When the deflection angle turns to zero, the classical differential cross section diverges due to the factor sin θ. This phenomenon is well known as the forward glory scattering [24]. The large cross section at $\theta_{cm} = 0$ for the one-electron capture reaction observed in the N^{5+} - He collisions is concluded to be due to the glory scattering, because the lower half of the deflection function shown in figure 8 passes through zero.

Another divergence of the cross section is observed when $|d\theta / db|^{-1} = 0$. Olson and Kimura [1] called this phenomenon 'inelastic rainbow' when they studied the differential cross section in the C^{6+} - H collisions.

This rainbow scattering is predicted to appear when the impact parameter $b = 5.1$, and the rainbow angle is – 0.171 rad, while the measured structure in figure 8 is located at $\theta_{cm} = 0.338$ rad. Though the agreement is not satisfactory, the overall structure is suitably reproduced. The rainbow angle changes considerably when the well depth of the model potential is increased. For example, the rainbow angle was calculated to be nearly equal to that measured when the well depth is increased by about 30 %. Therefore, the actual depth of the well is expected to be deeper than the model potential used.

The same calculation was made for the differential cross section measured at $E_{lab} = 47.5$ eV ($E_{cm} = 10.6$ eV) in the N^{5+} - He collisions. In this energy, θ_c was calculated to be 0.374 rad at $b = 6.85$, the deflection angle was zero at $b = 4.22$ and 5.56, and the rainbow angle was – 0.071 rad at $b = 4.8$. As the measured structure is located at 0.242 rad, the agreement is again far from quantitative, but the observed structures in the differential cross section are ascribed to the forward glory effect at $\theta_{cm} = 0$ and the second maximum is due to the inelastic rainbow.

Detailed theoretical calculations for the O^{5+} - He collisions based on the *ab initio* potentials were reported by Shimakura *et al* [12]. According to their results, the main reaction channel at low energies was reaction channel (7), which agrees well with the present assignment. The initial channel of this channel was assigned to the molecular state created during the collisions, 4Σ, and the final state was 2Σ. The initial state crosses with the 3Σ state at a large internuclear distance and, therefore, the crossing was reported to be almost diabatic. The transition to the final state occurs at the crossing point between 3Σ and 2Σ. Before this crossing

point, the 4Σ and 3Σ curves are almost flat, and 2Σ is always repulsive. Obviously, the deflection angles will be always positive and non-zero due to the repulsive character of these interaction potentials; consequently, no glory peak appears in the differential cross section in the O^{5+} - He system.

The critical angle θ_c for the one-electron capture process in the O^{5+} - He system at E_{lab} = 47.5 eV is assumed to be nearly equal to that calculated for the N^{5+} - He system at the same energy, because the exothermicity is nearly equal. The peak observed in figure 6 is located around θ_{cm} = 0.3 rad. This angle is smaller than 0.374 rad for the θ_c for the N^{5+} - He collisions at E_{lab} = 47.5 eV; hence, the peak observed in figure 6 is concluded to be the inelastic rainbow.

Our conclusion that no glory peak exists in the differential cross section for the one-electron capture process in the O^{5+} - He system disagrees with the interpretation of Waggoner *et al* [2]. Though it is hard to compare the results obtained at very different collision energies, it is worthwhile to point out a possible explanation of the origin of the two structures in their O^{5+} - He collisions observed at higher energies: The second structure probably correspond to the opening of different reaction channels. The candidate for such a reaction channel in the N^{5+} - He system is very limited, as reported by the measurements by Okuno *et al* [17], while other channels may exist in the O^{5+} - He system, as discussed by Kimura *et al* [13]. We could not clearly observe them in the present measurement for the O^{5+} - He collisions, but a weak indication of the peak shift to the higher energy side was detected at larger scattering angles. This is expected to correspond to the opening of the reaction channel (8) or (9). As reported in the differential cross sections for the F^{4+} - Ne collisions [26], a larger angular threshold was observed for the reaction channel with larger exothermicity.

We should point out that the collision mechanisms for the one-electron capture process in the N^{5+} - He and O^{5+} - He systems are very different but that the total cross sections determined by Ishii *et al* [27] were reported to be nearly identical at low energies. This might be explained by the fact that the exothermicities for both systems coincide accidentally. The location of the crossing points and the magnitude of the transition probabilities are expected to be so close to result in nearly equal total cross sections.

4. Summary

We have determined the relative state-selective differential cross sections for the one-electron capture process in the N^{5+} - He and O^{5+} - He systems below E_{lab} = 50 eV. The main reaction

channels are found to be $N^{5+}(1s^2\ ^1S) + He \rightarrow N^{4+}(1s^2 3s\ ^2S) + He^+ + 16.8$ eV and $O^{5+}(1s^2 2s\ ^2S) + He \rightarrow O^{4+}(1s^2 2s3p\ ^{1,3}P) + He^+ + 17$ eV. In the N^{5+} - He system, the differential cross section has a high peak at $\theta_{cm} = 0$, and the second peak appears at an angle that depends on the collision energy. By application of the classical trajectory analysis based on the reported *ab initio* potentials, we assign the peak that appears at $\theta_{cm} = 0$ to the forward glory effect, because of the existence of a shallow well in the interaction potential for the initial state. The second peak is assigned to the inelastic rainbow effect. As the interaction potentials corresponding to the reaction in the O^{5+} - He system are all repulsive character, the scattering angles are always positive and non-zero. No glory effect is detectable in the differential cross section, where only a single peak assignable to the inelastic rainbow is observed.

Acknowledgements

The author is grateful to Professor Kozo Kuchitsu for critical reading of the manuscript. This paper is dedicated to the late Dr. Kazumasa Ohtsuki, who gave me the idea of the analysis of the present results and his unpublished theoretical potentials. This work was partly supported by the Grant-in-Aid for Scientific Research (C) (17540373).

References

[1] Olson R E and Kimura M 1982 *J. Phys. B: At. Mol. Phys.* **15** 4231

[2] Waggoner W, Cocke C L, Tunnell L N, Havener C C, Meyer F W and Phaneuf R A 1988 *Phys. Rev.* A **37** 2386

[3] Andersson L R, Pedersen J O P, Bárány A, Bangsgaard J P and Hvelplund P 1989 *J. Phys. B: At. Mol. Opt. Phys.* **22** 1603

[4] Biedermann C, Cederquist H, Andersson L R, Levin J C, Short R T, Elston S B, Gibbons J P, Andersson H, Liljeby L and Sellin I A 1990 *Phys. Rev.* A **41** 5889

[5] Kamber E Y, Abu-Haija O and Wardwell J A 2008 *Phys. Rev.* A **77** 012701

[6] Hoshino M, Pichl L, Kanai Y, Nakai Y, Kitajima M, Kimura M, Li Y, Liebermann H P, Buenker R J, Tanaka H and Yamazaki Y 2007 *Phys. Rev.* A **75** 012716

[7] Cotte P H, Druetta M, Martin S, Denis A, Désesquelles J, Hitz D and Dousson S 1985 *Nucl.*

Instr. Meth. B **9** 743

[8] Dijkkampt D, Ćirić D, Vlieg E, de Boer A and de Heer F J 1985 *J. Phys. B: At. Mol. Phys.* **18** 4763

[9] Bacchus-Montabonel M C 1989 *Phys. Rev.* A **40** 6088

[10] Bacchus-Montabonel M C 1987 *Phys. Rev.* A **36** 1994

[11] Liu L, Zhao Y Q, Wang J G, Janev R K and Tanuma H 2010 *Phys. Rev.* A **81** 014702

[12] Shimakura N, Yamada S, Suzuki S and Kimura M 1995 *Phys. Rev.* A **51** 2989

[13] Kimura M, Iwai T, Kaneko Y, Kobayashi N, Matsumoto A, Ohtani S, Okuno K, Takagi S, Tawara T and Tsurubuchi S 1982 *J. Phys. B: At. Mol. Phys.* **15** L851

[14] Itoh Y 1994 *J. Phys. Soc. Japan* **63** 941

[15] Itoh Y 2002 *J. Phys. B: At. Mol. Opt. Phys.* **35** 3217

[16] Bischof G and Linder F 1986 *Z. Phys. D: At. Mol. Clusters* **1** 303

[17] Okuno K, Tawara H, Iwai T, Kaneko Y, Kimura M, Kobayashi N, Matsumoto A, Ohtani S, Takagi S and Tsurubuchi S 1983 *Phys. Rev.* A **28** 127

[18] Beijers J P M, Hoekstra R and Morgenstern R1994 *Phys. Rev.* A **49** 363

[19] Bangsgaard J P, Hvelplund P, Pedersen J O P, Andersson L R and Bárány A 1989 *Phys. Scr.* T **28** 91

[20] Morse F A and Bernstein R B 1962 *J. Chem. Phys.* **37** 2019

[21] Sobocinski P, Rangama J, Chesnel J-Y, Allio G, Hennecart D, Laurent G, Adoui L, Cassimi A, Dubois S, James O, Martina D, Spicq A, Bremer J-H, Dubois A and Frémont F 2003 *J. Phys. B: At. Mol. Opt. Phys.* **36** 1283

[22] Cederquist H, Andersen L H, Bárány A, Hvelplund P, Knudsen H, Nielsen E H, Pedersen J O K and Sørensen J 1985 *J. Phys. B: At. Mol. Phys.* **18** 3951

[23] Edens J, Kamber E Y, Akgüngör K and Ferguson S M 1996 *Nucl. Instr. Meth.* B **111** 27

[24] Child M S *MOLECULAR COLLISION THEORY* 1974 (London: Academic press) p 18

[25] Düren R 1973 *J. Phys. B: At. Mol. Phys.* **6** 1801

[26] Itoh Y and Ohtsuki K 2009 *J. Phys.: Conf. Ser.* **163** 012042

[27] Ishii K, Itoh A and Okuno K 2004 *Phys. Rev.* A **70** 042716